

PAPER

CVD-grown MoSe₂ with high modulation depth for ultrafast mode-locked erbium-doped fiber laser

To cite this article: Wenjun Liu *et al* 2018 *Nanotechnology* **29** 394002

View the [article online](#) for updates and enhancements.

Related content

- [Tungsten diselenide for mode-locked erbium-doped fiber lasers with short pulse duration](#)
Wenjun Liu, Mengli Liu, Yuyi OuYang et al.
- [Large-area and highly crystalline MoSe₂ for optical modulator](#)
Jinde Yin, Hao Chen, Wei Lu et al.
- [MoS₂ saturable absorber prepared by chemical vapor deposition method for nonlinear control in Q-switching fiber laser](#)
Meng-Li Liu, Yu-Yi OuYang, Huan-Ran Hou et al.



IOP | ebooks™

Bringing you innovative digital publishing with leading voices to create your essential collection of books in STEM research.

Start exploring the collection - download the first chapter of every title for free.

CVD-grown MoSe₂ with high modulation depth for ultrafast mode-locked erbium-doped fiber laser

Wenjun Liu^{1,2} , Mengli Liu¹, Yuyi OuYang¹, Huanran Hou¹, Ming Lei^{1,3} and Zhiyi Wei^{2,3}

¹ State Key Laboratory of Information Photonics and Optical Communications, School of Science, P. O. Box 122, Beijing University of Posts and Telecommunications, Beijing 100876, People's Republic of China

² Beijing National Laboratory for Condensed Matter Physics, Institute of Physics, Chinese Academy of Sciences, Beijing 100190, People's Republic of China

E-mail: mlei@bupt.edu.cn and zywei@iphy.ac.cn

Received 2 June 2018

Accepted for publication 3 July 2018

Published 19 July 2018



CrossMark

Abstract

Two-dimensional materials have been widely used as optical modulator materials in mode-locked fiber lasers. In terms of the performance of the fiber laser, one with an ultrashort pulse and high stability has great commercial value. Herein, the MoSe₂ grown by the chemical vapor deposition (CVD) method with high modulation depth, quality lattice structure and uniformity is successfully applied in a mode-locked erbium-doped fiber laser. The pulse duration and signal-to-noise ratio of the laser are 207 fs and 85 dB, respectively. The multifarious performance comparisons indicate that the CVD-based MoSe₂ saturable absorber with the tapered fiber structure has unique advantages not only in the generation of ultrashort pulses, but also in the optimization of laser stability.

Keywords: nonlinear optical materials, fiber lasers, saturable absorbers, mode-locked laser

(Some figures may appear in colour only in the online journal)

1. Introduction

Two-dimensional (2D) materials, as a class of saturable absorbers (SAs) with exotic nonlinear optical (NLO) properties, have drawn considerable attention to the generation of ultrashort pulses by means of passive mode-locking and Q-switching techniques [1–16]. Generally speaking, the NLO characteristics of materials rely heavily on the materials themselves. Since the discovery of graphene, researchers pay more attention to the investigation and application of new NLO 2D materials. Graphene enables an ultra-wide response due to its unique Dirac-like structure [17]. Meanwhile, the impressive NLO responses [18] (nonlinear refractive index $n_2 \sim 2 \times 10^{-7} \text{ cm}^2 \cdot \text{W}^{-1}$) of graphene play an important role in the effective modulation of light. Wavelength conversion

has also become an applied hotspot of graphene due to the strong Kerr nonlinearity [19]. The surface states structure of topological insulators (TI) is similar to graphene [20]. However, different from the small modulation depth of graphene [21], TI shows its advantages in large modulation depth [22]. Moreover, the large third-order NLO effects and broadband absorption characteristics of TI indicate that TI is a preeminent NLO material [23, 24]. Another 2D material, black phosphorus (BP), has its own layer-dependent direct bandgap (0.35–2 eV) [25, 26], which can be applied to the infrared communication band [27]. In general, the stability of BP is a major obstacle in its application. At present, plenty of methods are used to enhance the stability of BP and make it suitable as an SA material [28, 29].

In addition to the materials mentioned above, transition metal dichalcogenides (TMDs) have also been paid much attention in recent years due to their great potential in optical

³ Authors to whom any correspondence should be addressed.

and photonics applications [30]. Generally, numerous members of TMDs with similar structures and components are expressed as MX_2 , where M represents the transition metals (W, Mo, etc) and X represents elements in group VI (S, Se, Te, etc) [31, 32]. The inter-layer of the TMDs are combined with the weak van der Waals interaction while the intra-layer atoms are bound together by strong chemical bonds. Such a special combination enables the TMDs to be easily stripped into nanosheets to manufacture high-performance electronic devices [33, 34].

There are two main categories of TMDs that are receiving considerable attention, while the biggest difference between the two is the atomic weight of the chalcogenides. It is reported that sulfide-based TMDs have lighter chalcogenide atoms, which results in the increase of bandgap energy [35]. However, as the investigations generally concentrate on sulfide-based TMDs, the exploration of selenide-based TMDs are still at the initial stages. The bandgap of $MoSe_2$ is 1.09 eV [36], which indicates that it can not only be used in the visible wavelength regime, but also has great potential in the near infrared band [37, 38].

Generally speaking, the size and thickness of TMD films are important factors that affect the NLO response of materials, because undesired extrinsic crystal properties may cause inhomogeneities, impurities and defects [39, 40]. In comparison, the TMD film prepared by the chemical vapor deposition (CVD) method perform remarkably in uniformity and thickness control of the material, which is advantageous for the reduction of defects. Here, the $MoSe_2$ film grown by the CVD method is transferred onto a microfiber to form an SA. The small tapered waist diameter and long reaction length of the microfiber enables a full and effective light-matter interaction. Based on the NLO properties of the prepared $MoSe_2$ SA, the mode-locked erbium-doped fiber laser (EDFL) is successfully achieved. With this means, the 207 fs pulses with a signal-to-noise ratio (SNR) of 85 dB is generated. To the best of our knowledge, it is not only the shortest duration generated by $MoSe_2$ SA, but is also the most impressive compared to that of TMD-based EDFL.

2. Preparation and characterization of the $MoSe_2$ SA

In order to reduce undesired inhomogeneities, impurities and defects in the $MoSe_2$ films, the CVD method was adopted. Before synthesization, the clean SiO_2/Si substrates and full raw materials were already prepared. Along the direction of the air intake, the Se powder and MoO_3 powder were placed in the reaction chamber in turn. In particular, the MoO_3 powder was placed in the heating zone center. The SiO_2/Si substrate was placed at the end of the outlet, which was downstream of the MoO_3 powder. During synthesization, the flowing mixture gas mainly composed of H_2 and Ar (H_2 : 10 sccm, Ar: 65 sccm) assisted the admixture and reaction of the Se and MoO_3 vapors. To ensure the quality of the $MoSe_2$ films, the temperature in the furnace rose to 800 °C at a

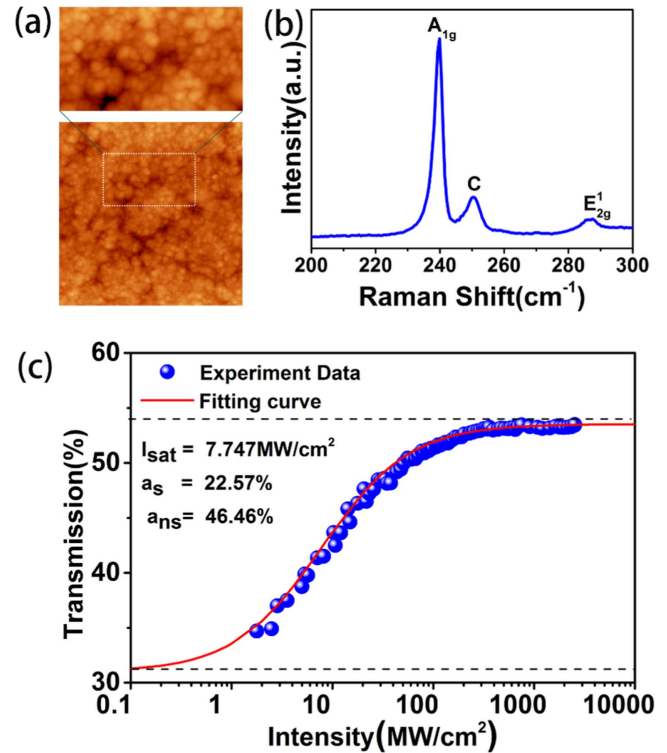


Figure 1. (a) The AFM of $MoSe_2$; (b) the Raman spectroscopy of $MoSe_2$; (c) the nonlinear response of $MoSe_2$ SA.

uniform rate of 15 °C min^{-1} . During the high temperature reaction of 25 min, the final product was carried to the substrate under the impetus of the mixed gas. After the natural cooling treatment, high quality $MoSe_2$ films were obtained. In general, the material attached on the substrate was inconvenient in application, free-standing nanosheets are preferred by comparison. Polymethyl methacrylate (PMMA) assisted the method as the mature and well-behaved technology has been widely used to achieve the stripping process for thin films. Therefore, the separation of the $MoSe_2$ films from the substrates was completing by using PMMA. After the spin coating and air drying, the $MoSe_2$ films were successfully stripped to have a complete lattice structure and good homogeneity. After treatment with acetone and deionized water, the remnants of PMMA were removed. The free-standing $MoSe_2$ films, which floated smoothly under the tension of water, were transferred to the tapered waist of the microfiber. In the process of migration, the microscope was employed to realize accurate micromanipulation. The microfiber with a tapered waist of 11 μm and a reaction length of 2.5 μm enabled a full and effective light-matter interaction.

Atomic force microscope (AFM) can not only detect the surface homogeneity of materials, but also measure film thickness accurately. The AFM image of the $MoSe_2$ films is shown in figure 1(a). When the measured area of $MoSe_2$ was $1 \times 1 \mu m$, uniform and compact particles were arranged in order, as seen in figure 1(a). The enlarged illustration in figure 1(a) further reflects the uniformity of the material. Meanwhile, the thickness of the $MoSe_2$ films was measured to

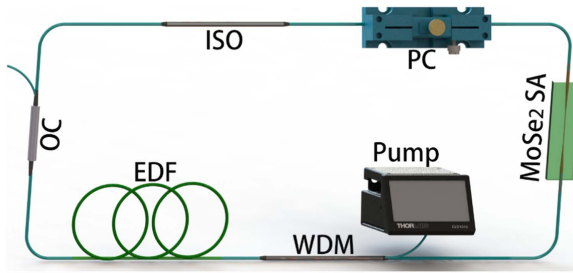


Figure 2. The experimental arrangement of MoSe₂-based EDFL.

be 9 nm. Raman spectroscopy is a common way of characterizing the mode of material vibration. From figure 1(b), there are two distinct peaks located at 239.9 cm⁻¹ and 286 cm⁻¹, respectively. According to previous research, the strong peaks at 239.9 cm⁻¹ correspond to the out-of-plane A_{1g} mode while the weak peaks at 286 cm⁻¹ correspond to the in-plane E_{2g}¹ mode [41–43]. The appearance of peak *c* is infrequent in previous characterization, we attribute it to Davydov splitting [44]. In addition, the saturable absorption is also an important feature of the material. In order to investigate the nonlinear response of MoSe₂ SA to light, the balanced twin detector measurement technology as a simple and effective method was successfully applied [45]. The light source employed in the measurement was a self-made mode-locked laser operating at 1550 nm with a pulse duration of 600 fs. After the fitting of the formula

$$\alpha(I) = \frac{\alpha_s}{1 + I/I_{sat}} + \alpha_{ns},$$

the saturable absorption parameter α_s , nonsaturable absorption parameter α_{ns} and saturation intensity I_{sat} were 22.57%, 46.46% and 7.747 MW cm⁻², respectively, as is presented in figure 1(c).

3. MoSe₂ mode-locked EDFL

MoSe₂ SA was employed in EDFL to investigate the saturable absorption characteristic, the simple experimental arrangement is shown in figure 2. As we can see, a common ring-type cavity was adopted. The 976/1550 nm wavelength division multiplexer (WDM) enabled light to be continuously pumped into the cavity. Under constant excitation of the pump, the erbium-doped fiber (EDF) consistently showed the amplification and enhancement of light. The isolator (ISO) prevented the propagation of undesired light propagation. To make the mode-locked laser operate at the optimum case, the polarization controller (PC) was employed to adjust the polarization state and birefringence in the cavity. The MoSe₂ SA was placed between the PC and WDM. The 80:20 output coupler enabled real-time monitoring of the laser data. 80% of light remained in the cavity to maintain a steady state of operation, whereas another 20% was exported. The data of the mode-locked sequence, spectrum and RF spectrum were collected by an oscilloscope (Tektronix DPO3054), optical spectrum analyzer (Yokogawa AQ6370C) and RF spectrum analyzer (Agilent E4402B).

4. Result and discussion

The mode-locked pulses were generated after appropriate optimization of the polarization and birefringence in the cavity by fine tuning the PC at a pump power of 630 mW. Through the monitoring of the oscilloscope, the mode-locked sequences displayed were stable and durable as is represented in figure 3(a). The inter-pulse time interval of the mode-locked pulses was measured to be 15.49 ns. During a long time of monitoring, the spectral changes in the different periods were recorded. From figure 3(b), we can see that the laser operated at 1552 nm with 3 dB bandwidth of 12.72 nm.

The autocorrelation trace of pulses indicate the characteristics of the pulse duration, which is the important parameter of the laser. To get the pulse duration, the data (blue dots) recorded in the experiment were fitted by the sech² function as indicated in figure 3(c). The pulse duration of 207 fs was not only the shortest duration generated by the MoSe₂ SA, but also impressive compared to that of the TMD-based EDFL. By the equation

$$TBP = \tau \times c \cdot \Delta\lambda/\lambda_0^2,$$

the time–bandwidth product (*TBP*) was able to be calculated theoretically. The parameter τ corresponds to the pulse duration, c is the speed of light in vacuum, $\Delta\lambda$ represents the 3 dB bandwidth and λ_0 is the center wavelength. Based on the recorded data, the *TBP* was calculated to be 0.3277. This is close to the theoretical value of 0.315, which indicates that the chirp in the cavity was slight. In the process of data collection, the laser consistently maintained stability and durability. In order to further prove the stability of the laser, the RF spectrum was a simple and persuasive method. From figure 3(d), the repetition rate of the pulse was 64.56 MHz. Both the uniform decline of frequency multiplication in illustration and the SNR of 85 dB indicate that the laser operated stably.

In order to make the content more convincing, the contrast experiment was supplemented. In the contrast experiment, the MoSe₂ SA was replaced by a tapered fiber of the same specification without any other materials while the other parts remained unchanged. However, the passively mode-locking phenomenon was not observed in the experiment. Therefore, the passively mode-locking phenomenon was in fact due to the MoSe₂.

The performance comparisons between the MoSe₂-based mode-locked EDFL and previous work are demonstrated in table 1. By comparison, the modulation depth of the CVD-based MoSe₂ SA is impressive, we attribute the good performance to the CVD method and tapered fiber structure of the MoSe₂ SA. The CVD method is mainly used to improve the uniformity of MoSe₂ films, and further improve the modulation depth of the MoSe₂ SA [46]. Compared to the MoSe₂ SA, which directly transfers the MoSe₂ to the cross-sectional area of the optical fiber, the fiber-taper WS₂ SA can achieve nonlinear control and better heat dissipation. By controlling the effective length of the fused zone and waist diameter of the tapered fiber, the nonlinearity of the MoSe₂ SA can be controlled. It has been reported that the waist diameter of the fiber-taper WS₂ SA is smaller, and the

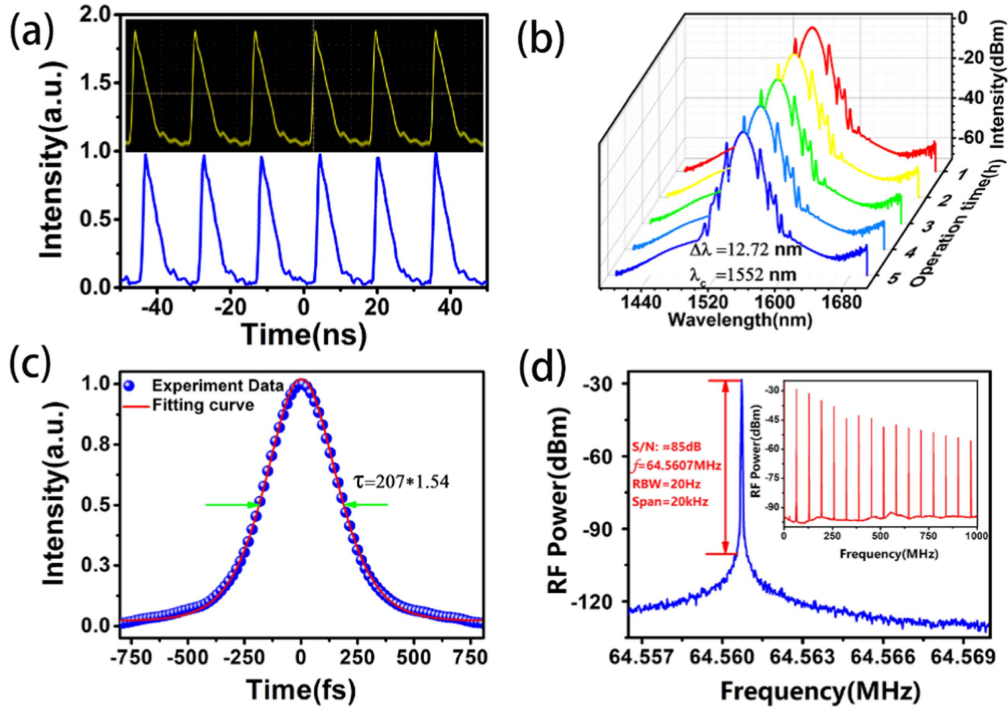


Figure 3. (a) The mode-locked sequence; (b) the spectral changes in different periods; (c) the autocorrelation trace of pulses; (d) the RF spectrum.

Table 1. Performance comparisons of mode-locked EDFL with MoSe₂ SA.

Materials	Fabrication	MD	$\lambda_0/\Delta\lambda$ (nm)	τ (fs)	SNR (dB)	Reference
PVA–MoSe ₂	LPE	5.4%	1557.3/5.4	798	59.1	[51]
SPF–MoSe ₂	LPE	1.4%	1557.1/2.3	1090	<60	[50]
PVA–MoSe ₂	LPE	0.4%	1562.6/2.2	1180	<60	[50]
PVA–MoSe ₂	LPE	7.3%	1560/7.8	580	50	[52]
PVA–MoSe ₂	LPE	0.63%	1558.25/1.76	1450	61.5	[38]
Microfiber–MoSe ₂	CVD	22.57%	1552/12.72	207	85	This work

effective length of the fused zone is longer, the nonlinearity of the SA will be stronger [47]. The strong nonlinearity characteristics of the SA may increase the modulation depth synchronously. Therefore, we think that the large modulation depth of the MoSe₂ SA is the result of the combination of the CVD method and tapered fiber structure. Moreover, because the contact area between the MoSe₂ films and optical fiber is large, it can be used to better heat dissipation and increase the operating threshold of the MoSe₂ SA. Furthermore, the pulse duration of the MoSe₂-based mode-locked EDFL in this work is shortest compared with that of other lasers. The large modulation depth may be the major reason for this phenomenon. In other words, under the same conditions, the large modulation depth is beneficial for the short pulse duration. In addition, the high SNR of the MoSe₂-based mode-locked EDFL indicates the stability of the operation. The stability of the laser is a parameter highly valued in commercial applications. The performance comparisons indicate that the CVD-based

MoSe₂ SA has unique advantages not only in the generation of ultrashort pulses, but also in the optimization of laser stability.

The direct bandgap of the monolayer MoSe₂ was 1.57 eV and the indirect bandgap of the bulk MoSe₂ was 1.1 eV according to previous research, which is way below the optical (excitonic) bandgap of MoSe₂ at 1550 nm [48]. Some different theories have been proposed to explain the governing mechanism, including two-photon absorption saturation, edges state of the materials and defect-induced bandgap decrease. In the theory of defect state, the defect of MoSe₂ is inevitable in the production process, which will influence its electronic and optical performance. It has been reported that the bandgap of MoS₂ and WS₂ can be significantly reduced by introducing the defects in a suitable range [49]. It is justifiable to believe the sub-bandgap saturable absorption of MoSe₂ is similar to the defect-induced bandgap decrease of MoS₂ and WS₂, because TMD materials possess similar lattice structures and photonic properties [50].

5. Conclusion

In conclusion, the CVD-based MoSe₂ SA has been successfully applied in mode-locked EDFL. Owing to the combination of the CVD method and the tapered fiber structure of the MoSe₂ SA, the prepared MoSe₂ SA has represented an impressive modulation depth of 22.57%. The obtained mode-locked EDFL not only has a short pulse duration of 207 fs, but also has an SNR of 85 dB. The TBP of 0.3277 indicates the chirp in the cavity is slight. The performance comparisons have indicated that the CVD-based MoSe₂ SA has unique advantages not only in the generation of ultrashort pulses, but also in the optimization of laser stability. As one of many promising materials, the CVD-based MoSe₂ has potential applications in further optoelectronic devices, and even commercial applications.

Acknowledgments

We acknowledge the financial support from the National Natural Science Foundation of China (NSFC) (Grant no. 11674036); the Beijing Youth Top-Notch Talent Support Program (Grant no. 2017000026833ZK08); the Fund of State Key Laboratory of Information Photonics and Optical Communications (Beijing University of Posts and Telecommunications, grant nos. IPOC2016ZT04, IPOC2017ZZ05).

ORCID iDs

Wenjun Liu  <https://orcid.org/0000-0001-9380-2990>

References

- [1] Liu W J, Liu M L, OuYang Y Y, Hou H R, Ma G L, Lei M and Wei Z Y 2018 Tungsten diselenide for mode-locked erbium-doped fiber lasers with short pulse duration *Nanotechnology* **29** 174002
- [2] Sobon G, Sotor J and Abramski K M 2012 Passive harmonic mode-locking in Er-doped fiber laser based on graphene saturable absorber with repetition rates scalable to 2.22 GHz *Appl. Phys. Lett.* **100** 161109
- [3] Hu G H et al 2017 Black phosphorus ink formulation for inkjet printing of optoelectronics and photonics *Nat. Commun.* **8** 278
- [4] Zhang M, Howe R C T, Woodward R I, Kelleher E J R, Torrisi F, Hu G H, Popov S V, Taylor J R and Hasan T 2015 Solution processed MoS₂-PVA composite for sub-bandgap mode-locking of a wideband tunable ultrafast Er: fiber laser *Nano Res.* **8** 1522–34
- [5] Zhang M, Hu G H, Hu G Q, Howe R C T, Chen L, Zheng Z and Hasan T 2015 Yb- and Er-doped fiber laser Q-switched with an optically uniform, broadband WS₂ saturable absorber *Sci. Rep.* **5** 17482
- [6] Chen B H, Zhang X Y, Wu K, Wang H, Wang J and Chen J P 2015 Q-switched fiber laser based on transition metal dichalcogenides MoS₂, MoSe₂, WS₂, and WSe₂ *Opt. Express* **23** 26723–37
- [7] Liu W J, Zhu Y N, Liu M L, Wen B, Fang S B, Teng H, Lei M, Liu L M and Wei Z Y 2018 Optical properties and applications for MoS₂-Sb₂Te₃-MoS₂ heterostructure materials *Photonics Res.* **6** 220–7
- [8] Liu W J, Pang L H, Han H N, Bi K, Lei M and Wei Z Y 2017 Tungsten disulfide for ultrashort pulse generation in all-fiber lasers *Nanoscale* **9** 5806–11
- [9] Bao Q L, Zhang H, Wang Y, Ni Z H, Yan Y L, Shen Z X, Loh K P and Tang D Y 2009 Atomic-layer graphene as a saturable absorber for ultrafast pulsed lasers *Adv. Funct. Mater.* **19** 3077–83
- [10] Yang H R and Liu X M 2018 WS₂-clad microfiber saturable absorber for high-energy rectangular pulse fiber laser *IEEE J. Sel. Top. Quant.* **24** 0900807
- [11] Chen H, Chen Y S, Yin J D, Zhang X J, Guo T and Yan P G 2016 High-damage-resistant tungsten disulfide saturable absorber mirror for passively Q-switched fiber laser *Opt. Express* **24** 16287–96
- [12] Wang J T, Jiang Z K, Chen H, Li J R, Yin J D, Wang J Z, He T C, Yan P G and Ruan S C 2017 Magnetron-sputtering deposited WTe₂ for an ultrafast thulium-doped fiber laser *Optics Lett.* **42** 5010–3
- [13] Yan P G et al 2017 Large-area tungsten disulfide for ultrafast photonics *Nanoscale* **9** 1871–7
- [14] Liu W J, Liu M L, Yin J D, Chen H, Lu W, Fang S B, Teng H, Lei M, Yan P G and Wei Z Y 2018 Tungsten diselenide for all-fiber lasers with the chemical vapor deposition method *Nanoscale* **10** 7971–7
- [15] Mao D, Zhang S L, Wang Y D, Gan X T, Zhang W D, Mei T, Wang Y G, Wang Y S, Zeng H B and Zhao J L 2015 WS₂ saturable absorber for dissipative soliton mode locking at 1.06 and 1.55 μm *Opt. Express* **23** 27509–19
- [16] Wu K, Guo C S, Wang H, Zhang X Y, Wang J and Chen J P 2017 All-optical phase shifter and switch near 1550 nm using tungsten disulfide (WS₂) deposited tapered fiber *Opt. Express* **25** 17639–49
- [17] Bonaccorso F, Sun Z, Hasan T and Ferrari A C 2010 Graphene photonics and optoelectronics *Nat. Photon.* **4** 611–22
- [18] Zhang H, Virally S, Bao Q L, Loh K P, Massar S, Godbout N and Kockaert P 2012 Z-scan measurement of the nonlinear refractive index of graphene *Opt. Lett.* **37** 1856–8
- [19] Xu B, Martinez A and Yamashita S 2012 Mechanically exfoliated graphene for four-wave-mixing-based wavelength conversion *IEEE Photon. Technol. Lett.* **24** 1792–4
- [20] Zhang H J, Liu C X, Qi X L, Dai X, Fang Z and Zhang S C 2009 Topological insulators in Bi₂Se₃, Bi₂Te₃ and Sb₂Te₃ with a single Dirac cone on the surface *Nat. Phys.* **5** 438–42
- [21] Zhang H, Bao Q L, Tang D Y, Zhao L M and Loh K P 2009 Large energy soliton erbium-doped fiber laser with a graphene-polymer composite mode locker *Appl. Phys. Lett.* **95** 141103
- [22] Chen S Q, Zhao C J, Li Y, Huang H H, Lu S B, Zhang H and Wen S C 2014 Broadband optical and microwave nonlinear response in topological insulator *Opt. Mater. Express* **4** 587–96
- [23] Yan P, Lin R, Chen H, Zhang H, Liu A, Yang H and Ruan S 2015 Topological insulator solution filled in photonic crystal fiber for passive mode-locked fiberlaser *IEEE Photonics Technol. Lett.* **27** 264–7
- [24] Yan P G, Lin R R, Ruan S C, Liu A J and Chen H 2015 A 2.95 GHz, femtosecond passive harmonic mode-locked fiber laser based on evanescent field interaction with topological insulator film *Opt. Express* **23** 154–64
- [25] Rudenko A N and Katsnelson M I 2014 Quasiparticle band structure and tight-binding model for single- and bilayer black phosphorus *Phys. Rev. B* **89** 201408
- [26] Tran V, Soklaski R, Liang Y F and Yang L 2014 Layer-controlled band gap and anisotropic excitons in few-layer black phosphorus *Phys. Rev. B* **89** 235319

- [27] Lu S B, Miao L L, Guo Z N, Qi X, Zhao C J, Zhang H, Wen S C, Tang D Y and Fan D Y 2015 Broadband nonlinear optical response in multi-layer black phosphorus: an emerging infrared and mid-infrared optical material *Opt. Express* **23** 11183–94
- [28] Guo Z N *et al* 2015 From black phosphorus to phosphorene: basic solvent exfoliation, evolution of Raman scattering, and applications to ultrafast photonics *Adv. Funct. Mater.* **25** 6996–7002
- [29] Guo Z N *et al* 2017 Metal-ion-modified black phosphorus with enhanced stability and transistor performance *Adv. Mater.* **29** 1703811
- [30] Wang Q H, Kalantar-Zadeh K, Kis A, Coleman J N and Strano M S 2012 Electronics and optoelectronics of two-dimensional transition metal dichalcogenides *Nat. Nanotechnol.* **7** 699–712
- [31] Pumera M, Sofer Z and Ambrosi A 2014 Layered transition metal dichalcogenides for electrochemical energy generation and storage *J. Mater. Chem. A* **2** 8981–7
- [32] Huang X, Zeng Z Y and Zhang H 2013 Metal dichalcogenide nanosheets: preparation, properties and applications *Chem. Soc. Rev.* **42** 1934–46
- [33] Novoselov K S, Jiang D, Schedin F, Booth T J, Khotkevich V V, Morozov S V and Geim A K 2005 Two dimensional atomic crystals *Proc. Natl Acad. Sci.* **102** 10451–3
- [34] Cunningham G, Lotya M, Cucinotta C S, Sanvito S, Bergin S D, Menzel R, Shaffer M S P and Coleman J N 2012 Solvent exfoliation of transition metal dichalcogenides: dispersibility of exfoliated nanosheets varies only weakly between compounds *ACS Nano* **6** 3468–80
- [35] Tiu Z C, Ahmad H, Zarei A and Harun S W 2016 Generation of multi-wavelength erbium-doped fiber laser by using MoSe₂ thin film as nonlinear medium and stabilizer *Chin. Opt. Lett.* **14** 041901
- [36] Kumar A and Ahluwalia P K 2012 Electronic structure of transition metal dichalcogenides monolayers 1H-MX₂ (M = Mo, W; X = S, Se, Te) from ab-initio theory: new direct band gap semiconductors *Eur. Phys. J. B* **85** 186
- [37] Luo Z Q, Li Y Y, Zhong M, Huang Y Z, Wan X J, Peng J and Weng J 2015 Nonlinear optical absorption of few-layer molybdenum diselenide (MoSe₂) for passively mode-locked soliton fiber laser *Photonics Res.* **3** A79–86
- [38] Woodward R I, Howe R C T, Runcorn T H, Hu G, Torrisi F, Kelleher E J R and Hasan T 2015 Wideband saturable absorption in few-layer molybdenum diselenide (MoSe₂) for Q-switching Yb-, Er- and Tm-doped fiber lasers *Opt. Express* **23** 20051–61
- [39] Zhou K G, Zhao M, Chang M J, Wang Q, Wu X Z, Song Y and Land Zhang H L 2015 Size-dependent nonlinear optical properties of atomically thin transition metal dichalcogenide nanosheets *Small* **11** 694–701
- [40] Trushin M, Kelleher E J R and Hasan T 2016 Theory of edge-state optical absorption in two-dimensional transition metal dichalcogenide flakes *Phys. Rev. B* **94** 155301
- [41] Tongay S, Zhou J, Ataca C, Lo K, Matthews T S, Li J, Grossman J C and Wu J 2012 Thermally driven crossover from indirect toward direct bandgap in 2D semiconductors: MoSe₂ versus MoS₂ *Nano Lett.* **12** 5576–80
- [42] Xia J, Huang X, Liu L Z, Wang M, Wang L, Huang B, Zhu D D, Li J J, Gu C Z and Meng X M 2014 CVD synthesis of large-area, highly crystalline MoSe₂ atomic layers on diverse substrates and application to photodetectors *Nanoscale* **6** 8949–55
- [43] Chang Y H *et al* 2014 Monolayer MoSe₂ grown by chemical vapor deposition for fast photodetection *ACS Nano* **8** 8582–90
- [44] Kim K, Lee J U, Nam D and Cheong H 2016 Davydov splitting and excitonic resonance effects in Raman spectra of few-layer MoSe₂ *ACS Nano* **10** 8113–20
- [45] Liu W J, Pang L H, Han H N, Liu M L, Lei M, Fang S B, Teng H and Wei Z Y 2017 Tungsten disulfide saturable absorbers for 67 fs mode-locked erbium-doped fiber lasers *Opt. Express* **25** 2950–9
- [46] Wei R, Zhang H, Tian X, Qiao T, Hu Z, Chen Z, He X, Yu Y and Qiu J 2016 MoS₂ nanoflowers as high performance saturable absorbers for an all-fiber passively Q-switched erbium-doped fiber laser *Nanoscale* **8** 7704–10
- [47] Khazaiezhad R, Kassani S H, Jeong H, Park K J, Kim B Y, Yeom D and Oh K 2015 Ultrafast pulsed all-fiber laser based on tapered fiber enclosed by few-layer WS₂ nanosheets *IEEE Photonic. Tech. L.* **27** 1581–4
- [48] Wu K *et al* 2018 High-performance mode-locked and Q-switched fiber lasers based on novel 2D materials of topological insulators, transition metal dichalcogenides and black phosphorus: review and perspective *Opt. Commun.* **406** 214–29
- [49] Wang S X, Yu H H, Zhang H J, Wang A Z, Zhao M W, Chen Y X, Mei L M and Wang J Y 2014 Broadband few-layer MoS₂ saturable absorbers *Adv. Mater.* **26** 3538–44
- [50] Mao D, She X Y, Du B B, Yang D X, Zhang W D, Song K, Cui X Q, Jiang B Q, Peng T and Zhao J L 2016 Erbium-doped fiber laser passively mode locked with few-layer WSe₂/MoSe₂ nanosheets *Sci. Rep.* **6** 23583
- [51] Koo J, Park J, Lee J, Jhon Y M and Lee J H 2016 Femtosecond harmonic mode-locking of a fiber laser at 3.27 GHz using a bulk-like, MoSe₂-based saturable absorber *Opt. Express* **24** 10575–89
- [52] Ahmad H B, Aidit S N, Hassan N A, Ismail M F and Tiu Z C 2016 Generation of mode-locked erbiumdoped fiber laser using MoSe₂ as saturable absorber *Opt. Eng.* **55** 076115